MOLECULAR CARCINOGENESIS 45:490–505 (2006)

Expression of Heregulin by Mouse Mammary Tumor Cells: Role in Activation of ErbB Receptors

M. Schmitt,[1] M.P. Walker,[1] R.G. Richards,[1] W.P. Bocchinfuso,[2] T. Fukuda,[1] D. Medina,[3] F.S. Kittrell,[3] K.S. Korach,[1] and R.P. DiAugustine[1]*

[1]*Laboratory of Molecular Carcinogenesis, National Institute of Environmental Health Sciences, Research Triangle Park, North Carolina*
[2]*Laboratory of Reproductive and Developmental Toxicology, National Institute of Environmental Health Sciences, Research Triangle Park, North Carolina*
[3]*Department of Cell Biology, Baylor College of Medicine, Houston, Texas*

The inappropriate activation of one or more members of the ErbB family of receptor tyrosine kinases [ErbB-1 (EGFR), ErbB-2, ErbB-3, ErbB-4] has been linked with oncogenesis. ErbB-2 is frequently coexpressed with ErbB-3 in breast cancer cells and in the presence of the ligand heregulin (HRG) the ErbB-2/ErbB-3 receptors form a signaling heterodimer that can affect cell proliferation and apoptosis. The major goal of the present study was to determine whether endogenous HRG causes autocrine/paracrine activation of ErbB-2/ErbB-3 and contributes to the proliferation of mammary epithelial tumor cells. Tyrosine-phosphorylated (activated) ErbB-2 and ErbB-3 receptors were detected in the majority of extracts from tumors that had formed spontaneously or as a result of oncogene expression. HRG-1 transcripts and protein were found in the epithelial cells of most of these mouse mammary tumors. Various mouse mammary cell lines also contained activated ErbB-2/ErbB-3 and HRG transcripts. A ~50 kDa C-terminal fragment of pro-HRG was detected, which indicates that the HRG-1 precursor is readily processed by these cells. It is likely that the secreted mature HRG activated the ErbB-2/3 receptors. Addition of an antiserum against HRG to the mammary epithelial tumor cell line TM-6 reduced ErbB-3 Tyr-phosphorylation. Treatment with HRG-1 siRNA oligonucleotides or infection with a retroviral construct to stably express HRG siRNA effectively reduced HRG protein levels, ErbB-2/ErbB-3 activation, and the rate of proliferation, which could be reversed by the addition of HRG. The cumulative findings from these experiments show that coexpression of the HRG ligand contributes to activation of ErbB-2/Erb-3 in mouse mammary tumor cells in an autocrine or paracrine fashion. Published 2006 Wiley-Liss, Inc.†

Key words: tyrosine phosphorylation; proteolytic cleavage; proliferation

INTRODUCTION

The ErbB receptors are important in organ development and in the pathogenesis of various malignancies, such as breast cancer. These proteins belong to subclass I of the superfamily of receptor tyrosine kinases. The ErbB family has four members: epidermal growth factor receptor (ErbB-1), ErbB-2, ErbB-3, and ErbB-4 (summarized in Lupu et al., 1995 [1]). ErbB-3 is deficient in tyrosine kinase activity because of a substitution of key amino acids in the cytoplasmic domain [2]. Multiple ErbB ligands, which generally originate as transmembrane precursors, have been discovered, with each having specific affinities for the different ErbBs [3,4]. These ligands bind the extracellular domain of the ErbB receptors, which, in turn, causes receptor homo- or heterodimerization [2,5,6]. A specific ligand for ErbB-2 has not been identified; however, heterodimerization of ErbB-2 with other ErbBs readily occurs (summarized in Lupu et al., 1995 [1]) and increases the affinity of the respective ligand to its receptor [7]. Evidence for functional ErbB interactions has come from in vitro [8] and in vivo [9] studies. There are various isoforms of the ligand heregulin (HRG) that specifically bind ErbB-3 or ErbB-4 and stimulate heterodimerization with ErbB-2 [summarized in 10]. ErbB-2 mediates the transphosphorylation of ErbB-3 [6], which creates docking sites for downstream signaling molecules. For instance, ErbB-3 has multiple binding sites for the p85 subunit of phosphatidylinositol-3-kinase (PI3-K) [11].

Overexpression of ErbB-2 occurs in 25–30% of human breast cancers and is usually associated with a poor prognosis (summarized in Hynes and Stern,

Abbreviations: cDNA, complementary DNA; DMEM, Dulbecco's Modified Eagle Medium; EGF, epidermal growth factor; FBS, fetal bovine serum; HRG, heregulin; kDa, kilo Dalton; MMTV, mouse mammary tumor virus; PBS, phosphate-buffered saline; PCR, polymerase chain reaction; PI3-K, phosphatidylinositol-3-kinase; P-Tyr, Phosphotyrosine; RT-PCR, reverse transcriptase PCR; siRNA, small interfering RNA; Wt, wild-type.

*Correspondence to: Mail Drop D4-04, NIEHS, NIH, P.O. 12233, Research Triangle Park, N.C. 27709.

Received 4 October 2005; Revised 17 November 2005; Accepted 29 November 2005

DOI 10.1002/mc.20180

1994 [12]). Several studies have reported the coexpression of ErbB-3 and ErbB-2 in human breast cancer [13–16]. Experiments have shown that the signals that emanate from the ErbB-2/ErbB-3 heterodimer can promote breast tumor cell division [summarized in 1] and tumor development [13]. This is in accord with earlier studies where ErbB-2 (Wt) and ErbB-3 were shown to cooperate in transformation of fibroblasts [17]. MMTV-Neu (Wt) transgenic mice that overexpress ErbB-2 in the mammary gland develop mammary epithelial tumors after a median latency period of about 200 d [18], but mice transgenic for human ErbB-3 under a MMTV-promoter do not exhibit an increased occurrence of mammary tumors [19]. The potential importance of ErbB-2 and ErbB-3 in breast cancer progression has prompted investigation of the functional properties of the HRG ligand. Previous studies have shown that 30–60% of human breast carcinomas were positive for HRG when analyzed by Northern blots [20]. Several reports showed that HRG has an antiproliferative role and can promote cell differentiation or apoptosis [20–24]. These findings were contradicted by other studies showing no effect on proliferation or even a mitogenic effect of HRG. This ligand stimulated proliferation of SKBr3 cells, which have ErbB-3 receptors and an abundance ($>10^6$ receptors/cell) of ErbB-2. HRG-1β stimulated proliferation of various human malignant breast epithelial cells in vitro. The proliferative response in this study was directly correlated with the number of ErbB-2 receptors, even in those cases where the number of ErbB-3 receptors/cell was $<10^3$. In this same study, exogenous HRG also stimulated an increase in the size of several tumors derived from these cell lines and implanted in nude mice [25]. Transfection of human breast cancer MDA-MB-435 cells with a HRG-expressing construct increased the size of the tumors at the inoculation site and stimulated metastasis of these cells to the lungs [26]. In a more recent study, MCF-7 cells were transfected with HRGβ2 cDNA and inoculated in the mammary fat pad of ovariectomized nude mice. Expression of HRG promoted preneoplastic transformation of adjacent mouse mammary tissue [27]. Endogenous production of HRG in MMTV-HRGβ2 transgenic mice, repeatedly bred to maximize expression of the ligand by the mammary epithelium, caused mammary adenocarcinomas at a median age of ~1 yr [28]. In spite of extensive research, it is currently unclear what factors determine whether HRG-1 acts as a mitogen or promotes cell death and differentiation.

The major objective of the present study was to examine mouse mammary tumors and cell lines for activation of ErbB-2 and ErbB-3 and determine if this activation could be attributed to autocrine/paracrine action of the HRG ligand. Different strategies were used to compromise the activity or synthesis of the HRG ligand in mouse mammary cells in order to determine if it drives ErbB-2/ErbB-3 tyrosine phosphorylation and cell proliferation. Our findings indicate that the HRG ligand is expressed with a high frequency by mouse mammary tumor cells and that the ligand in situ contributes to activation of ErbB-2/ErbB-3 and cell proliferation.

MATERIALS AND METHODS

Animals and Tumors

Housing and procedures with mice that were used for collection of normal and tumorous mammary tissues followed the guidelines of the National Institute of Environmental Health Sciences (NIEHS) Animal Care and Use Committee. MMTV- Wnt-1 hemizygous transgenic mice [29] were a gift of Dr. Harold Varmus (Memorial Sloan-Kettering Cancer Institute, New York, NY). MMTV-Neu (activated) hemizygous transgenic mice [30] were obtained from Dr. Phil Leder, Harvard University Medical School, Boston, MA and Dr. G. Rao, NIEHS. ErbB-2 overexpressing MMTV-Neu (Wt) homozygous mice transgenic on the FVB background were obtained from The Jackson Laboratory, Bar Harbor, ME and allowed to undergo multiple pregnancies. Tumor samples were collected several weeks after the last pregnancy. Tumors arose after transplanting the TM2L, TM2H, TM4, TM10, TM40D, and EL-12-0D cell lines, which were developed by one of the authors (D. M.), into cleared fat pads of syngenic hosts. Chemically induced mouse mammary tumors were obtained through the NIEHS National Toxicology Program and the Laboratory of Experimental Pathology: Mammary adenocarcinomas formed spontaneously (n = 1) or after treatment with codeine (n = 3), ethylnitrosourea (n = 1), methylene chloride (n = 3), nickel sulfate (n = 2), vinyl carbamate (n = 1), vanadium pentoxide (n = 1), nickel subsulfide (n = 1), and t-butylhydroquinone (n = 1). Two fibroadenomas were also included in the study: One had formed after trichloropropane treatment and one spontaneously. Four sarcomas that had formed after treatment with 1,3-butadiene (n = 3) or *p*-nitrobenzoic acid (n = 1), were also included. Palpable mammary tumors at approximately 1 cm in diameter as well as normal mammary glands were either chilled and used immediately for analysis of ErbB receptor tyrosine kinases, or snap-frozen in N_2 and stored at −80°C for subsequent extraction of RNA, or fixed in 10% phosphate-buffered formalin at 4°C for 1 d followed by immersion in ethanol at 4°C for 24 h prior to embedding into paraffin.

Cell Culture Conditions for Mammary Epithelial Cell Lines

The Neu(Wt)-overexpressing mammary tumor cell line NT-2 was a generous gift from Dr. R. T. Reilly, John Hopkins University School of Medicine, Baltimore, MD. The cells were cultured under the conditions described [31]. TM-6 and TM40D cells

were established as previously stated [32]. Both cell lines were grown in DMEM/F-12 (1:1) supplemented with 15 mM HEPES, 10 μg/mL insulin, 5 ng/mL EGF, 5% FBS, 100 U/mL penicillin, 100 μg/mL streptomycin, and 0.5 μg/mL amphotericin. The COMMA-D cell line was derived from normal mammary gland [33] and was a generous gift from Dr. Gloria Jahnke, NIEHS, Research Triangle Park. COMMA-D cells were grown in DMEM/F-12 (1:1) supplemented with 5% FBS, 5 μg/mL insulin, and 50 μg/mL gentamycin. All cells were maintained at 37°C in 5% CO_2 and passaged once a week. Where applicable, cells were stimulated in the absence of serum or growth factors with HRG-1β (EGF-domain, recombinant, from Upstate, Lake Placid, NY).

Inhibition of ErbB-1 Kinase

Confluent dishes of TM-6 cells were washed twice with DMEM/F-12 and exposed to serum- and growth-factor free medium. After 24 h, 250 pM of PD153035 (Calbiochem, San Diego, CA) or vehicle was added and cells were incubated for another 24 h. Total protein was extracted and subjected to BCA assay (Pierce, Rockford, IL). ErbB receptor activation was determined after immunoprecipitation of the respective ErbB and blotting for P-Tyr. Toxicity of the inhibitor was evaluated with the CellTiter 96 AQ_{ueous} One Solution Cell Proliferation Assay (Promega, Madison, WI).

Pro-HRG Antiserum

The Ab pro-HRG-CT-1 rabbit antiserum was made to the C-terminal region of human pro-HRG-1: A peptide corresponding to the amino acids 615–640 of pro-HRG [34] was custom synthesized (Princeton BioMolecules, Langhorne, PA) and coupled to ovalbumin (Calbiochem, La Jolla, CA) by the glutaraldehyde method.

Protein Extracts, Immunoprecipitation, and Immunoblotting

Protein from cultured cells was extracted by incubating confluent cultures for 15 min on ice with solubilization buffer (1% Triton X-100, 0.25% sodium deoxycholate, 150 mM NaCl, 1 mM Na_3VO_4, 1 mM NaF, 50 mM Na_2MoO_4, 20 μg/mL aprotinin, 20 μg/mL leupeptin, and 4 μg/mL 4-amido-phenylmethylsulfonyl fluoride in 50 mM Tris-HCl, pH 7.4). Extracts of mammary tumors or glands were prepared with this buffer as previously described [9]. After homogenization, aliquots of mammary extracts containing equal amounts of protein were added to solubilization buffer without sodium deoxycholate and subjected to immunoprecipitation as described in [9] using 5 μg of rabbit-anti-ErbB-1 (described in [9]), −ErbB-2 (C-18), or −ErbB-3 (C-17) antibody (both from Santa Cruz Biotechnology, Santa Cruz, CA). Immunoprecipitates were washed three times with solubilization buffer without sodium deoxycholate, reduced in Laemmli sample buffer [35], and resolved by 4–20% SDS-PAGE (Bio-Rad Laboratories, Hercules, CA), and transblotted to Immobilon-P (Millipore, Bedford, MA) membrane. The membrane was blocked with either 5% bovine serum albumin/Tris-buffered saline containing 0.1% Tween 20 or 3% nonfat dry milk/Tris-buffered saline and probed with antisera to the following proteins: P-Tyr (monoclonal; horseradish peroxidase-conjugated; ICN, Costa Mesa, CA), ErbB-2, ErbB-3 (see above), pro-HRG (Ab pro-HRG-CT-1; see above), the EGF-like domain of HRG (Ab-2; rabbit polyclonal; NeoMarkers, Fremont, CA), the p85-subunit of PI3-K (rabbit polyclonal; Upstate, Lake Placid, NY, cat. no. 06-195), ErbB-1 (see above), pan-cytokeratin (mouse monoclonal; Calbiochem, San Diego, CA), glyceraldehyde-3-phosphate dehydrogenase (mouse monoclonal; Chemicon International, Temecula, CA, cat. no. MAB374), and actin (C-14; goat polyclonal; Santa Cruz Biotechnology). In control sample, the specific antiserum used for immunoblotting was omitted and substituted with an appropriate preimmune serum or immunoglobulin fraction. The blots were probed with the appropriate secondary antisera conjugated to horseradish peroxidase, and immunoreactive proteins were detected as described earlier [9].

Immunohistochemistry

Tissue samples were cut into 4 μm sections. Following rehydration, sections were treated with 18% H_2O_2 in methanol and washed with 1× Automation Buffer (Biomedia Corp., Foster City, CA). Sections were then reacted with 0.05 mg/mL trypsin (Sigma, St. Louis, MO) in PBS for 5–10 min, washed, and blocked with 10% normal goat serum (Vector Laboratories, Burlingame, CA). Primary antisera were diluted as stated below in 10% normal goat serum and applied for 1 h: pro-HRG (Ab pro-HRG-CT-1; 1:2000, see above), HRG (Ab-1; 1:20; rabbit polyclonal; NeoMarkers), ErbB-3 (1:25, see above), and ErbB-2 (1:50, see above). Specificity of the reaction was shown by coincubation of the antisera with 2 mg/mL of the respective blocking peptide and by omission of the antisera. Incubation with the primary antiserum was followed by treatment with 1:400 biotinylated goat anti-rabbit IgG (Vector Laboratories) for 30 min. After washing, the sections were reacted with 1:400 ABC reagent (Vector Laboratories) for 30 min, washed, and then covered with DAB + H_2O_2 solution. After rinsing in deionized water, the sections were counterstained with toluidine blue and dehydrated with graded alcohols. Photographs were taken with a SPOT digital camera (Diagnostic Instruments, Inc., Sterling Heights, MI) attached to a Zeiss ECLIPSE E600 microscope.

Extraction of RNA, RT-PCR

Mammary tissues were excised, weighed, and then homogenized on ice in TRIzol® (1 mL per 50–100 mg

of tissue) (Invitrogen, Carlsbad, CA) with an OMNI International TH115 power homogenizer (3 bursts full power, each 10 s). RNA was extracted according to the manufacturer's instructions and dissolved in 100 μl diethylpyrocarbonate (DEPC)-treated water. Reverse transcriptase (RT)-PCR (RT-PCR) was carried out using a Gene Amp PCR System 9700 (Applied Biosystems, Foster City, CA) and the SuperScript First-Strand Synthesis System (Invitrogen): 1 μl total RNA (~2 μg) was reverse transcribed with oligo$(dT)_{12-18}$ primers according to the manufacturer's instructions. An aliquot (1 μl) of the reaction solution was added to a mix containing 10× PCR buffer (2.5 μl), 25 mM $MgCl_2$ (1.5 μl), 10 mM dNTPs (0.5 μl), 0.1 mM specific oligonucleotide primers (0.25 μl each), 1 U of Platinum™ Taq (5 U/μl), DMSO (1.25 μl), and DEPC water (17.55 μl) to give a final reaction volume of 25 μl (all reagents were from Invitrogen). Cycle conditions were 94°C (denaturation) for 30 s; 58°C (annealing) for 40 s; and 72°C (extension) for 1 min. Forward (F) and reverse primers (R) of HRG-1 [36,37] and cyclophilin [38] used for RT-PCR were: HRG-1Fseq: 5′-TGTCAGCCTCAACTGAAAG-A-3′; HRG-1Rseq: 5′-ATTGATTCACCAGTTGCACA-3′; CycloF: 5′-ATAAGGGTTCCTCCTTTCAC-3′; CycloR: 5′-CAATGTTCATGCCTTCTTTC-3′. Thirty cycles were used for all primer pairs. After amplification, products (expected size 519 bp) were resolved by electrophoresis in 3% Synergel-Agarose (Diversified Biotech, Boston, MA) gels and visualized with ethidium bromide. Amplified product was not observed in these tumor samples when reverse transcriptase was omitted. The RNA integrity of these tumor samples was confirmed by assessment of ribosomal RNA by gel electrophoresis and amplification of mouse cyclophilin transcripts.

Downregulation of HRG-1 by siRNA

For transient downregulation of HRG, siRNA oligonucleotides were designed to target the region common to all HRG-1 splice forms (NCBI acc. no. NM_178591) utilizing the SMARTpool algorithm (Dharmacon, Lafayette, CO). HRG silencing by the SMARTpool as well as by individual siRNA oligonucleotides (sequences available upon request) was validated by quantitative PCR, immunofluorescence, and Western blotting. Successful transfection of TM-6 cells was determined by using a fluorescein-labeled luciferase GL2 siRNA duplex (Dharmacon, Lafayette, CO) and analyzing the transfection efficiency after 1–2 d by trypsinizing and washing the cells twice with PBS and determining their fluorescence by flow cytometry, as compared with non-transfected cells. As a positive control for silencing, luciferase GL2 siRNA was co-transfected with the pGL2-luciferase plasmid (Dharmacon, Lafayette, CO); luciferase activity could be reduced by ~99%. We ruled out toxicity resulting from the transfection conditions by using the CellTiter 96 Aqueous One Solution Cell Proliferation Assay (Promega). The HRG siRNA oligonucleotide concentration yielding optimal silencing was determined by quantitative real-time PCR: 1 d after plating 4.3×10^5 TM-6 cells per 35-mm-dish, cells were transfected and RNA was extracted with the RNeasy kit (Qiagen, Valencia, CA). Silencing was detectable with as little as 5 nM siRNA. Best results were achieved with 2.8 μg of siRNA (corresponding to a final concentration of 100 nM siRNA) and 4.5 μl TransIT-TKO (Mirus, Madison, WI). The sequence that yielded the most pronounced silencing effect in the transient assay (5′-GAGCT-GAACCGTAGGAATA-3′) and a scramble sequence (5′-GCGCGCTTTGTAGGATTCG-3′) were used to create stable siRNA constructs according to the instructions by BD Biosciences (Mountain View, CA). Polyacrylamide gel electrophoresis (PAGE) purified complementary ssDNA oligonucleotides (Sigma-Genosys, The Woodlands, TX) were annealed (95°C, 2 min) in a buffer containing 10 mM Tris, pH 7.5, 50 mM NaCl, and 1 mM EDTA and then brought to room temperature. The DNA Ligation Kit Version 2 (TaKaRa, Madison, WI) was used to ligate the resulting dsDNA inserts into the pSIREN-RetroQ Vector linearized with *Bam*HI and *Eco*RI (BD Biosciences). The ligation reaction was carried out for 1 h at 16°C with 25 μg linearized plasmid DNA and 10 pmoles of annealed insert. After the ligation, the resulting plasmid was transformed into competent *E. coli* XL_1 blue by a standard protocol [39]. The resulting colonies were screened for carrying the correct insert by restriction digestion with *Swa*I (New England Biolabs, Ipswich, MA) and by sequencing with the DYEnamic ET mix (Amersham, Piscataway, NJ) and the sequencing primer 5′-CTTGAACC-TCCTCGTTCGACC-3′. The sequencing products were cleaned up with the Dye ex 2.1 kit from Qiagen (Valencia, CA) and analyzed as described above.

Plasmid Construction and Transfection Into Cultured Cells

The plasmid for the expression of human ErbB-2 (pcDNA3.1 human ErbB-2) was kindly provided by Dr. K. L. Carraway III, University of California Davis Cancer Center, Sacramento, CA. The plasmid containing the human ErbB-3 cDNA fragment (pCEV29 ErbB3) was kindly provided by Dr. S. A. Aaronson, Mount Sinai Medical Ctr., NY), and subcloned into the multiple cloning site of pcDNA3.1 (pcDNA3.1 human ErbB-3). To conserve the function of the PDZ domain of ErbB-2 and ErbB-3, the short DNA fragments that encode the HA (ErbB-2) and FLAG (ErbB-3) tag were introduced after the N-terminal signal peptide. The predicted amino acid sequence after the introduction is GAASTQ(aa19-24)-YPYDYP-DYA(HA tag)-TQVCTGT for ErbB-2, and ARGSE-V(aa17-21)-DYKDDDDK(FLAG tag)- EVGNSQ for

ErbB-3. The tag sequences were introduced by Quick change PCR system (Stratagene, La Jolla, CA) and corresponding oligonucleotides. All coding regions of the cDNAs were confirmed by cycle sequencing reaction. The sequences used for tag insertion and sequencing reactions are available on request. The human cDNA of ErbB-3 was excised from pCEV29 ErbB-3 and subcloned into the *Xho*I site of LXIN (Clontech, PaloAlto, CA) after a blunting reaction. The direction of the cDNA was confirmed by sequencing and a restriction digest of the plasmid.

TM-6 or COMMA-D cells were plated at a concentration of 4.4×10^5 cells per 60-mm dish. TM-6 cells were transfected using 3 μg of DNA and 8.7 μl of TransIT-TKO (Mirus), and COMMA-D cells with 7.4 μg of DNA and 6.2 μl Fugene 6 (Roche, Indianapolis, IN). A cell population enriched for expressing ErbB-2 or the empty control vector was obtained by selection with Geneticin (Invitrogen). ErbB-2 overexpression was compared to the control-transfected cells by Western blotting, with actin or GAPDH as a loading control.

Retroviral Infection and Selection of Cultured Cells

The recombinant retroviral plasmids were introduced into PT67 packaging cells (BD Biosciences) with Fugene 6 (Roche) based on the manufacturer's protocol. Stably transfected PT67 cells were selected with 1 mg/mL G418 (ErbB3) or 2 μg/mL puromycin (Sigma) and expanded. The target cells were infected by the method provided by BD Biosciences. After the infection, the COMMA-D cells were selected with 200 μg/mL G418, and the TM-6 cells were selected with 1 mg/mL G418 or 6 μg/mL puromycin. The surviving cells were expanded and used as enriched population, except in the case of the pSIREN-HRG-siRNA transfectants, where several colonies were isolated.

Quantitative Real-Time PCR

RNA was extracted with the RNeasy Mini Kit (Qiagen, Valencia, CA). A DNA removal step using DNAse I was included. RNA was reverse transcribed as described above. Quantitative real-time PCR was performed from 1 μl cDNA solution with the SYBR Green PCR Master Mix (Applied Biosystems, Foster City, CA). The primers for HRG-1 were 5′-CCCTGGCTGACTCTGGAGAA-3′ (forward) and 5′-GGTGATGTTGGCAGAGGCA-3′ (reverse), and the primers for β-actin were 5′-GACAGGATGCAGAAG-GAGATTACTG-3′ (forward) and 5′-GCTGATCCA-CATCTGCTGGAA-3′ (reverse). After denaturation at 94°C for 10 min, the cDNAs were amplified for 40 cycles on the ABI Prism 7900 HT (Applied Biosystems). Cycle conditions were 95°C for 15 s and 60°C for 1 min. Changes in HRG-1 expression were calculated from C_t-values obtained for HRG-1 after normalization with β-actin.

Immunofluorescence Staining

TM-6 cells were detached with 0.25% trypsin-EDTA (Invitrogen) and fixed with Cytofix/Cytoperm solution (BD Biosciences) at 4°C for 20 min. Cells were centrifuged for 10 min at 4000 rpm in a microfuge. 1×10^6 cells were subjected to each staining reaction: After fixation, cells were washed twice with 1 mL Perm/Wash (BD Biosciences). Nonspecific binding sites were blocked by incubating the cells with 10% goat serum in Staining Buffer (BD Biosciences) at 4°C for 15 min and with 200 μg/mL goat-IgG in Staining Buffer at 4°C for 15 min. After one wash step with Perm/Wash, cells were incubated with the primary antibody rabbit-anti-pro-HRG (C-20; Santa Cruz Biotechnology) or with rabbit-IgG at a concentration of 8 μg/mL in Staining Buffer at 4°C for 1 h. To prove specificity, 0.8 μg/mL of the primary antibody was preincubated overnight at 4°C with 4 μg/mL of the corresponding blocking-peptide (amino acids 615–640). After two wash steps, cells were incubated in the dark with the secondary antibody goat-anti-rabbit-IgG AlexaFlour-488 (Molecular Probes, Eugene, OR) at 4°C for 20 min at a concentration of 1 μg/mL in Staining Buffer. After two wash steps with Perm/Wash, cells were suspended in 1 mL PBS and analyzed with a Becton-Dickinson LSR flow Cytometer (San Jose, CA) equipped with CellQuest software. Ten thousand cells per sample were analyzed for AlexaFluor-488 fluorescence.

Cell Cycle Analysis

Cells (6×10^5) were harvested after 3 d of incubation by trypsinization. Cell cycle analysis was performed as previously described [40] with a BD Biosciences FACSort flow cytometer (San Jose, CA) equipped with CellQuest software.

RESULTS

Activated ErbB-2/3 Receptor Tyrosine Kinases in Mouse Mammary Tumors

ErbB-2/3 expression and activation were investigated in mouse mammary adenocarcinomas that originated from the transgenic models MMTV-Neu (Wt) and MMTV-Wnt-1 or formed spontaneously or after carcinogen-treatment (for details see Materials and Methods). ErbB receptors were immunoprecipitated from extracts and then analyzed by immunoblotting. As shown in Figure 1, bands corresponding to ErbB-1, ErbB-2, and ErbB-3 were readily detected in the MMTV-Wnt-1 [29] mammary tumor extracts. The amount of receptor protein in the tumors was increased and compared with extracts of mammary glands from nontransgenic adult virgin females. ErbB immunoprecipitates from the Wnt-1 mammary tumors revealed positive bands when blotted for P-Tyr. In contrast, normal adult virgin mammary glands revealed low levels of ErbB-2 and ErbB-3 expression with no detectable P-Tyr immunoreactivity

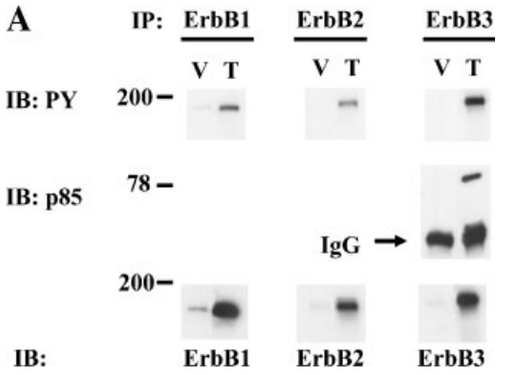

Figure 1. Tyrosine phosphorylation of ErbB-1, ErbB-2, and ErbB-3, and binding of the p85 regulatory subunit of PI3-K to ErbB-3 in mammary glands of wild-type adult virgin mice (V) or mammary tumors (T) of Wnt-1 transgenic mice. Tissue extracts were analyzed by immunoprecipitation of ErbB-1, ErbB-2, and ErbB-3 with subsequent immunoblotting (IB) for phosphotyrosine (PY), p85, ErbB-1, ErbB-2, or ErbB-3. The data are representative of five separate trials.

(Figure 1). As a confirmation of ErbB-3 activation in the Wnt-1 mouse tumors, immunoprecipitates of this receptor were also analyzed for the p85 PI3-K regulatory subunit. As shown in Figure 1, a strong p85 signal was detected in the ErbB-3 precipitates of the Wnt-1 tumor samples; a p85 band was not apparent in ErbB-3 precipitates from normal adult virgin mammary gland.

Analysis of mammary tumor extracts from the MMTV-Neu (Wt) transgenics [18] revealed the expected high levels of ErbB-2 protein; however, the extent of Tyr-phosphorylation of this receptor varied among samples. ErbB-3 was detected in all nine MMTV-Neu (Wt) tumor extracts analyzed and was activated, as determined by both Tyr-phosphorylation and p85-recruitment to the receptor. The level of activation of ErbB-3 in these extracts appeared to correlate directly with the level of receptor protein (data not shown).

ErbB-2-expression among tumors generated by injecting mice with various tumorigenic mammary epithelial cell lines [32] varied from weak in TM40D- and EL-12-0D-derived tumors to moderate in TM2L-, TM2H-, TM4-, and TM10-derived tumors. In most samples, ErbB-2-expression and P-Tyr levels correlated. ErbB-3 expression also varied considerably among this collection of tumors from barely detectable in EL-12-0D- to very strong in TM4-derived tumors. ErbB-3 phosphorylation and p85 recruitment to ErbB-3 correlated for the most part with the ErbB-3-expression levels (data not shown). In summary, ErbB-2- and ErbB-3 expression varied more among the transplanted tumors than it did among either of the transgenic models.

A relatively high epithelial content may contribute to the observed elevated expression of tumor ErbB-2/3 when compared to that of the normal mammary gland. To account for this, sample loading was adjusted for cytokeratin. We found that levels of both ErbB-2 and ErbB-3 varied considerably among the different tumors. These levels, in some cases, were comparable or even less than those of the virgin gland (data not shown). Thus, the expression of ErbB-2/3 in the tumors appears to be determined by both epithelial content and variability in cell expression levels.

ErbB2 was readily detectable by immunohistochemistry in the cytoplasm of most epithelial cells of both normal virgin mammary glands and tumor tissues. ErbB-3 was detected in some ductal epithelial cells of virgin mammary glands. The staining was generally weak and occurred in a granular pattern in the luminal aspect of the cytoplasm. In contrast, the epithelial cells of the tumors displayed a strong and rather uniform staining for ErbB-3 in the cytoplasm. In some cells, immunostaining occurred in the nucleus (Figure 2A). The signal intensity was not evenly distributed throughout the tissue.

Expression of HRG by Mouse Mammary Tumors

The detection of activated ErbB-2/3 in mouse mammary tumors suggested that the HRG ligand is present. To determine if this was the case, RNA was extracted and evaluated for HRG-1 transcripts by RT-PCR. Oligonucleotide primers flanking the EGF-like and transmembrane domains (primer set IIseq) should detect transcripts of the α and β isoforms of HRG-1 [41]. In mammary glands obtained from adult virgin female mice, there was only a very faint band visible after RT-PCR analysis; in contrast, glands obtained from pregnant mice (day 18) revealed a much higher level of HRG-1 transcript (Figure 3A). HRG-1 transcripts were also readily detected at the predicted size in all Wnt-1 transgenic mouse mammary tumors (Figure 3A). PCR-products representing amplified HRG-1 mRNA were also clearly visible when RNA from MMTV-Neu (Wt) tumors was analyzed. A variety of other mouse mammary tumors, mostly adenocarcinomas and adenomas (see Materials and Methods), were examined for HRG mRNA. These included tumors from MMTV-Neu (activated) transgenic mice as well as tumors that developed spontaneously, from transplanted cell lines or as a consequence of exposure to chemicals. Among the 32 tumors analyzed, all but 3 were positive for HRG transcripts. Only the adenocarcinoma that arose after t-butylhydroquinone treatment and both of the fibroadenomas were HRG-negative. It is possible that HRG expression is mostly associated with epithelial-derived mammary tumors.

Immunoblots of lysates from tumors and virgin glands were evaluated with an antiserum to pro-HRG-1 (Ab pro-HRG-CT-1), with protein loading adjusted for cytokeratin expression. The immunoblots revealed bands at ~45 and 50 kDa in the case of the normal gland. Lysates of MMTV-Neu (Wt and

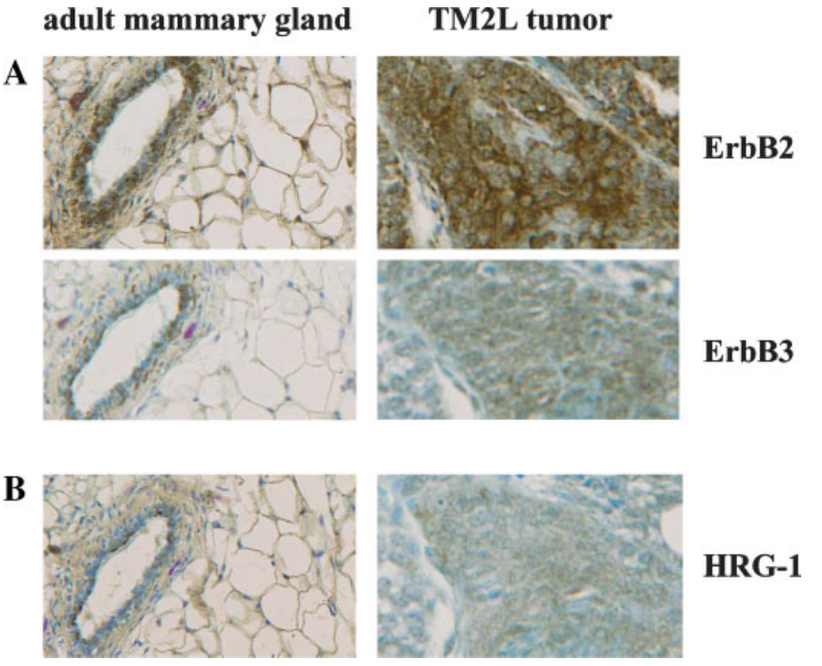

Figure 2. Localization of ErbB-2, ErbB-3, and heregulin-1 to epithelial cells of adult virgin mammary glands and mammary tumors. Representative serial sections from an adult virgin (Wt) mammary gland and the transplanted mammary epithelial tumor TM2L were reacted with antisera to ErbB-2 or ErbB-3 (A), or the extreme C-terminus of pro-heregulin-1 (HRG-1) (B). Sections were counterstained with toluidine blue. Magnification: ×40.

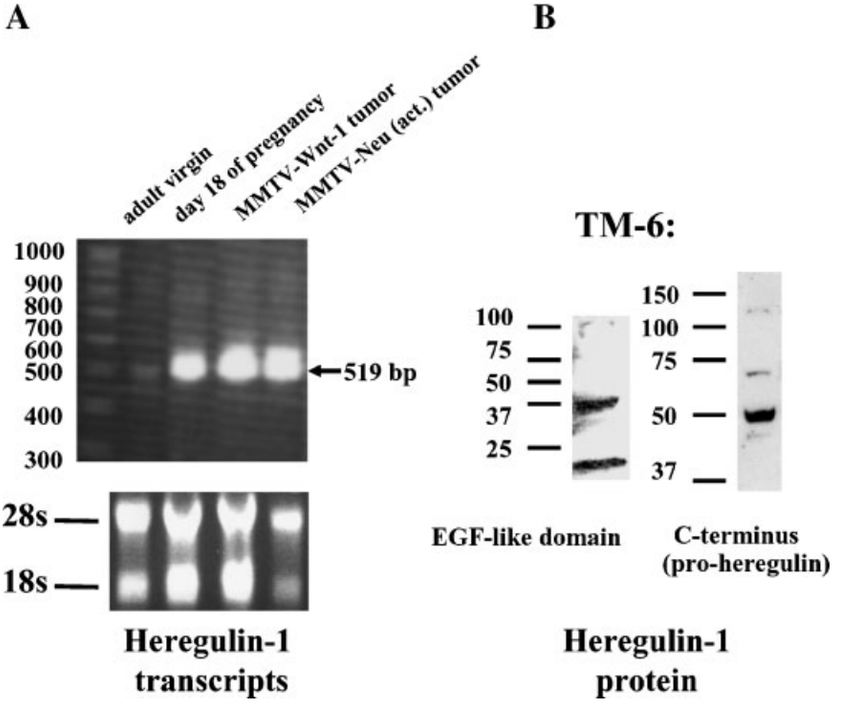

Figure 3. Detection of heregulin-1 in mammary epithelial cells. (A) Heregulin-1 mRNA was amplified by RT-PCR, and PCR-products were analyzed by agarose gel electrophoresis. Integrity of the RNA was demonstrated by agarose gel electrophoresis of total RNA; bands for the 28s- and the 18s-rRNA are visible. Nucleic acids are visualized under UV light by ethidium bromide. (B) TM-6 cells were grown to near confluence and lysates analyzed by immunoblotting. Blots were probed with the Ab-2 antibody against the EGF-like domain of heregulin-1 or with Ab-pro-HRG-CT-1 against the extreme C-terminal domain of pro-heregulin-1. Representative blots are shown.

activated) and MMTV-Wnt-1 tumors produced bands that were stronger than those of the virgin gland. Most tumor samples displayed additional bands: A particularly strong band was seen at ~37 kDa. In contrast, when the blot was probed with an antibody that detects the EGF-like domain of HRG (Ab-2), most tumor lysates gave only a weak signal at ~45 kDa, and several bands between 30 and 50 kDa (data not shown).

Immunolocalization with the Ab pro-HRG-CT-1 antiserum was used to confirm the expression of the HRG-1 in situ. Occasional cells in the epithelium of the virgin gland were weakly positive. The signal localized to the cytoplasm, primarily near the lumen (Figure 2B). A second antiserum (Ab-1), which detects the extracellular domain of HRG-1, confirmed this staining pattern in the rodent mammary gland. In sections of the tumors obtained from the MMTV-Neu (Wt) and MMTV-Wnt-1 animals (data not shown) and from the transplanted tumors (Figure 2B), positive immunostaining with the Ab pro-HRG-CT-1 antibody was present in the cytoplasm of nearly all epithelial cells observed. The staining intensity within most tumor sections varied. Generally, the HRG-immunoreactivity appeared stronger in the tumors than in the normal gland. In all tumor samples, the staining was cytoplasmic and concentrated along the cell borders. Immunostaining was barely detectable or negative in cells that comprised the mammary lymph node.

ErbB-2/3 Activation and HRG Expression in Mouse Mammary Epithelial Cell Lines

The combined presence of activated ErbB-2/3 and HRG-1 in most of the tumor samples led us to consider that endogenous HRG-1 is responsible for or contributes to the ErbB-2/3 activation. In order to conduct functional studies, we selected several mammary epithelial cell lines representative of the diverse backgrounds our tumor samples were derived from. The NT-2 cell line was established from a tumor that formed in an MMTV-Neu (Wt) transgenic mouse [31]. The TM-6 and the TM40D cell lines, when transplanted into host animals, form hyperplastic outgrowths, which eventually give rise to distinct tumors [32]. COMMA-D cells have been derived from normal mammary gland tissue [33]. The epithelial character of these cell lines has been shown in part by others, and been confirmed by us by their ability to express cytokeratin. While all four cell lines have Tyr-phosphorylated ErbB-1 and ErbB-2, NT-2 cells, as expected, have the highest ErbB-2 activation levels. ErbB-3 was present and constitutively phosphorylated in NT-2, COMMA-D, and TM-6 cells. ErbB-4 was below detection level of Western blots (<100 μg protein per lane) in all cell lines but NT-2, where there was a very weak signal. The data are summarized in Table 1. The ErbB-3 ligand, HRG-1, was found

Table 1. Expression and Activation of ErbB Receptors and Heregulin-1 in Mouse Mammary Epithelial Cell Lines

	ErbB-1 expression	ErbB-1 PY	ErbB-2 expression	ErbB-2 PY	ErbB-3 expression	ErbB-3 PY	p85-binding to ErbB3	ErbB-4 expression	Heregulin-1 expression
COMMA-D	++	+	++	+	+	+	+	−	+
NT-2	+	+	+++	++	+++	++	+	+	++
TM40D	++	+	+	+	−	−	−	−	+
TM-6	+++	+	++	+	++	+	+	−	++

−, undetectable; +, weak signal; ++, moderate signal; +++, strong signal when up to 100 μg of protein were analyzed by Western blotting.

in all four cell lines with similar levels in NT-2 and TM-6 cells, but at slightly lower expression levels in TM40D and COMMA-D cells, as determined by Western blotting with Ab pro-HRG-CT-1 (Table 1). TM-6 cell extracts displayed a prominent band at ~50 kDa; additional weaker bands were visible at about 45, 70, and 110 kDa. When TM-6 lysates were immunoblotted with the Ab-2 antibody that detects the EGF-like domain of HRG-1, multiple bands were evident, primarily at ~20 and 35 kDa (Figure 3B). HRG-1 transcripts could be amplified by RT-PCR in all cell lines (data not shown). Thus, these cell lines represent a situation similar to the mouse mammary tumors concerning their ErbB and HRG-1 status.

Since the cell lines already express HRG-1, we wanted to determine whether added ligand would influence ErbB3-activation. When TM-6 cells were exposed to 10 ng/mL HRG-1β for 15 min, ErbB-2/3 phosphorylation was not further increased. HRG treatment had no significant effect on TM-6 cell proliferation when cells were counted after 3 or 6 d of incubation (data not shown). COMMA-D cells, however, displayed a twofold increase in ErbB-3 phosphorylation when stimulated with 10 ng/mL HRG-1β or 100 ng/mL HRG-1α (data not shown).

Influence of Altered ErbB-2 or ErbB-3 Expression or ErbB-1 Kinase Activity on Mammary Epithelial Cell Lines

Since the ErbB-3 receptor was constitutively phosphorylated in TM-6 and COMMA-D cells and could not be further activated by HRG-1 in TM-6, we wondered if ErbB-3 was maximally stimulated in these cells. Therefore, we investigated if increasing the amount of ErbB-3 would allow for further ErbB-3 activation. After each of the cell lines was engineered to overexpress ErbB-3, both ErbB-3 protein levels and ErbB-3/ErbB-2 phosphorylation increased in COMMA-D (Figure 4A) and TM-6 cells, whereas ErbB-2 expression was not upregulated. When the ErbB-3 overexpressing COMMA-D cells were stimulated with HRG-1β for 15 min, they showed a moderate increase in ErbB-3 phosphorylation. ErbB-3 phosphorylation intensity was back to control levels after 4 h, and reduced to 50% of control levels after 24 h (Figure 4B). No such changes were seen in TM-6 cells (data not shown). Neither the overexpression of ErbB-2 nor ErbB-3 caused significant changes in HRG expression in any of the cell

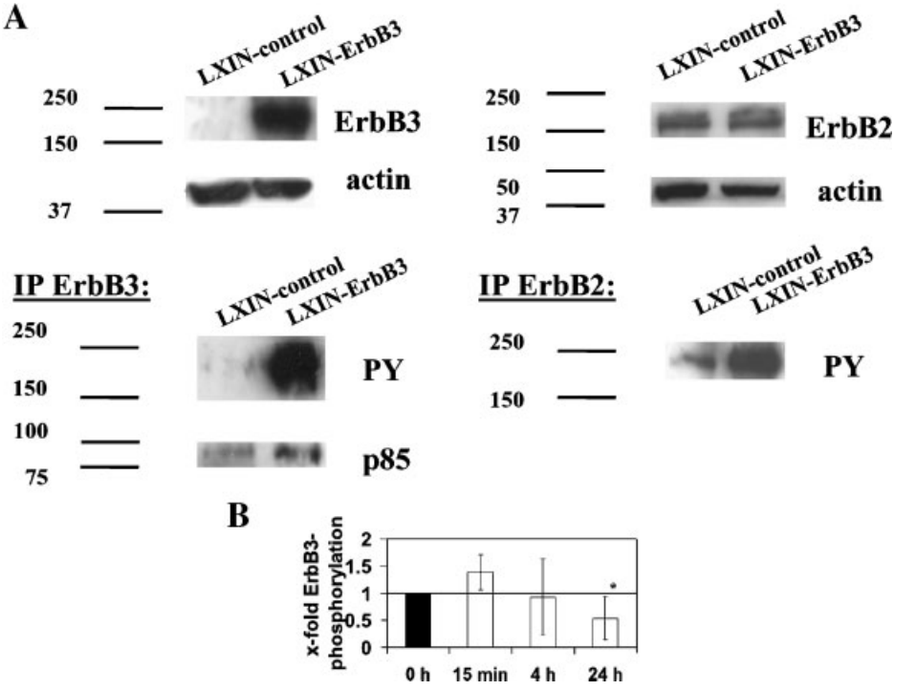

Figure 4. Impact of ErbB-3-overexpression on ErbB-2 and ErbB-3 expression/activation. (A) COMMA-D cells were stably transfected with an ErbB-3 expression plasmid or the empty LXIN-control vector. Cells were grown in serum-free medium for 24 h before lysis. ErbB-2 and ErbB-3 expression was analyzed by Western blotting; actin served as loading control. ErbB-2 and ErbB-3 were immunoprecipitated (IP) and immunoblotted for phosphotyrosine (PY) and the p85-subunit of PI3-K. Blots are representative of two (IP ErbB-2) or four (IP ErbB-3) individual experiments. (B) ErbB-3 overexpressing COMMA-D cells (COMMA-D-LXIN-ErbB3) were washed twice with DMEM/F-12 and then grown in serum-free medium for 24 h prior to treatment. Cells were stimulated with 10 ng/mL heregulin-1β for various periods as indicated. ErbB-3 was precipitated from lysates and blots were probed with anti-phosphotyrosine. Autoradiography films were analyzed by densitometry with ScionImage software. Changes to untreated controls were calculated from two (15 min, 4 h) or seven (24 h) individual experiments; bars represent SD. (*) Significantly different from control-treated: $P = 0.011$.

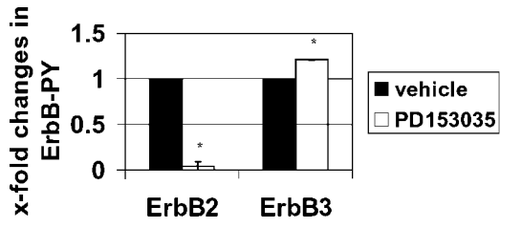

Figure 5. Effects of the ErbB-1 kinase inhibitor PD153035 on ErbB-2 and ErbB-3 tyrosine phosphorylation. TM-6 cells were grown in serum-free medium for 24 h, then treated with 250 pM PD153035 or vehicle for 24 h. ErbB-2 and ErbB-3 were immunoprecipitated from cell lysates. Blots were probed for phosphotyrosine (PY). Autoradiography films were scanned and signal intensity was analyzed with the ScionImage software. Changes in ErbB-2 or ErbB-3 tyrosine phosphorylation of the PD153035-treated cells compared with the vehicle-treated cells were calculated. The data are summarized from two separate trials; bars represent SD. (*) significantly different from vehicle-treated: ErbB-2, ErbB-3: $P < 0.0001$.

lines evaluated when analyzed by Western blotting with the Ab pro-HRG-CT-1 antibody (data not shown).

Although ErbB-2 is the preferred heterodimerization partner for ErbB-3, dimerization and activation of ErbB-3 by ErbB-1 is possible [11,42]. When TM-6 cells were treated with the ErbB-1 kinase inhibitor PD153035, ErbB-2 phosphorylation was markedly reduced, however, neither ErbB-3 (Figure 5) nor ErbB-1 (data not shown) phosphorylation were decreased by the inhibitor.

Influence of HRG Bioavailability/Synthesis on ErbB-2/3 Activation

Since the cells constitutively synthesized HRG-1, and exogenously added HRG had little influence on ErbB2/3 activation or cell growth, we compromised endogenously produced HRG-1 in TM-6 cells by two different methods. As a first approach, we treated TM-6 cells with the antibody Ab-2, which should compromise binding of the ligand to ErbB-3. After 12 h of incubation, precipitates of ErbB3 revealed a 50% reduction in Tyr-phosphorylation when compared to controls (Figure 6).

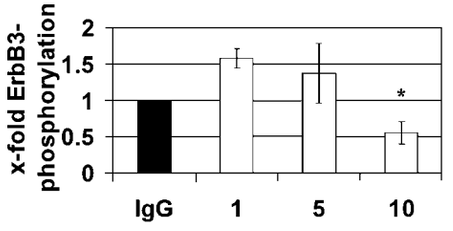

Figure 6. Influence of a heregulin-neutralizing antibody on ErbB-3 tyrosine phosphorylation. Confluent cultures of TM-6 cells were washed twice with DMEM/F-12 and then incubated with serum-free medium for 24 h. The medium was replaced again with fresh serum-free medium prior to treatment with the heregulin-1 neutralizing antibody Ab-2 at the concentrations [μg/mL] indicated, or with the respective concentrations of normal rabbit immunoglobulin (IgG) for 12 h. Proteins were extracted and ErbB-3 was immunoprecipitated from cell lysates. Blots were probed for phosphotyrosine. Autoradiography films were scanned and signal intensity was analyzed with the ScionImage software. The data are summarized from three separate trials; bars represent SE. (*) Significantly different from control-treated; 10 μg/mL Ab-2: $P = 0.05$.

As a second experimental approach, we employed RNAi techniques to decrease endogenous HRG-1. Four siRNA oligonucleotides were designed as described in Materials and Methods to target all known isoforms of HRG-1. Each of the four oligonucleotides, as well as their equimolar mixture, decreased HRG-1 mRNA-expression significantly in TM-6 cells by ~50% compared to scramble-sequence transfected cells, as measured by quantitative real-time PCR. The downregulation of HRG-1 mRNA was detectable as early as 24 h after transfection. The silencing effect weakened after 4 d (Figure 7A). Although 5 nM siRNA oligonucleotides caused a significant decrease of HRG-1 mRNA, the most pronounced silencing effect was achieved with 100 nM siRNA oligonucleotides. Immunofluorescence staining revealed that 100 nM HRG-1 siRNA did not decrease HRG-1 protein before day 3 following transfection. The siRNA oligonucleotide 1 with the sequence 5′-GAGCTGAACCGTAGGAATA-3′ (position 226) proved to be the most powerful and caused a 50% decrease of HRG-1 protein. The HRG-1 downregulation was not restricted to a particular subpopulation (Figure 7B). Similarly, a 50% decrease in HRG-1 protein was seen after two rounds of transfection with this sequence, when protein was extracted 4 d after transfection and analyzed by Western blotting (data not shown). ErbB-3-Tyr-phosphorylation was decreased by 20% following siRNA treatment for 4 d (Figure 7C), whereas no decrease in ErbB-3 expression was observed. In order to overcome the transient nature of the silencing effect, TM-6 cells were stably transfected with a retroviral construct expressing this particular sequence. The downregulation of HRG-1 was not as pronounced as with the transient transfection (Figure 8A). Still, we could see a decrease of ErbB-3 phosphorylation (Figure 8B); ErbB-2 phosphorylation was decreased by ~30% (Figure 8C). The changes in ErbB-2 phosphorylation could not be attributed to changes in expression levels. Two clones of the HRG-1 siRNA-expressing TM-6 cells that showed the best HRG-1 knock-down (#1 and #7) both showed a reduced cell proliferation rate: After 6 d, the cell numbers were reduced to 30% (Figure 9A) and 40% (data not shown), respectively, of control transfected cells, which correlated with a decrease of TM-6-pSIREN-HRG#1 cells in S-phase to one-third (Figure 9B). HRG-1β (100 ng/mL) restored cell growth to the levels of control-transfected cells (Figure 9A), proving specificity of the HRG-1 siRNA.

DISCUSSION

In the present study, we examined the premise that coexpression of the HRG ligand and ErbB-2/ErbB-3 receptors provides a functional autocrine/paracrine system in mouse mammary cancer cells.

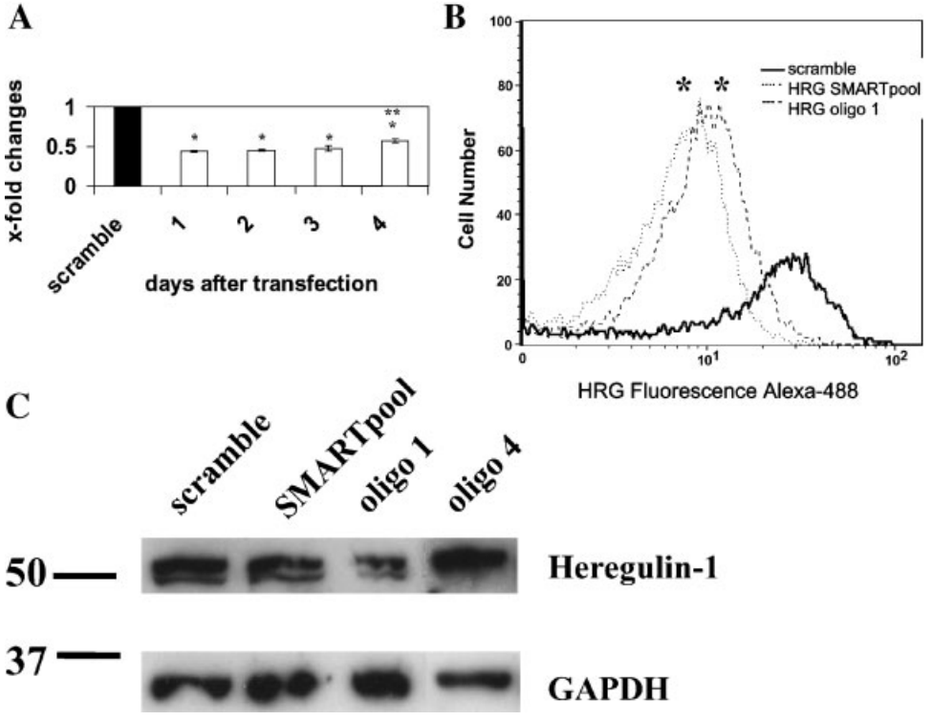

Figure 7. Decrease of heregulin-1 expression by transfection with specific heregulin-1 siRNA sequences. (A) TM-6 cells were transfected with the heregulin-1-specific oligo 4 or the scramble siRNA duplex. RNA was extracted after 1–4 d and changes in heregulin-1 mRNA expression were evaluated by quantitative real-time PCR. Data of a representative experiment are shown; averages were calculated from 5 (heregulin) or 2 (actin) individual data points and expressed as x-fold changes from scramble-transfected controls; bars represent SE. (*) significantly different from controls, all $P < 0.0001$; (**) different from 1–3-d treated. (B) TM-6 cells were transfected with the heregulin-1-specific (HRG) oligo 1, the equimolar mixture of all four oligos (SMARTpool), or the scramble siRNA duplex. After 3 d, heregulin-1 expression was assessed by immunofluorescence and cells were analyzed by flow cytometry. Data of a representative experiment are shown. (*) different from controls. (C) TM-6 cells were twice transfected within a 2-d interval with the heregulin-1-specific oligo 1 (HRG siRNA) or a scramble sequence as described in Materials and Methods. Twenty-four hours after the second transfection, cells were switched to serum-free medium. Four days after the initial transfection, cell lysates were prepared, ErbB-3 was immunoprecipitated, and blots were probed for phosphotyrosine (PY). Autoradiography films were scanned and signal intensity was analyzed with the ScionImage software. The data from two separate trials are summarized; bars represent SD. (*) Significantly different from control-transfected cells; $P = 0.0166$.

The frequent occurrence of HRG ligand expression along with activated ErbB-2 and ErbB-3 in tumor samples supports the hypothesis that this system operates in the microenvironment of the tumor. Furthermore, the results from immunolocalization studies suggest that ligand and receptors colocalize in tumor epithelial cells, creating a favorable proximity for ligand/receptor interaction. Finally, the endogenously produced HRG-1 was shown to activate the ErbB-2/ErbB-3 heterodimer constitutively and drive cell proliferation in a mammary cancer cell line derived from one of these tumors.

Several lines of evidence of our in vivo and cell culture data support the notion that ErbB-2 and ErbB-3 function as a heterodimer: In the vast majority of tumors analyzed, coactivation of ErbB-2 and ErbB-3 was detectable. Secondly, in COMMA-D and TM-6 cells, overexpression of ErbB-3 resulted in increased ErbB-2 activation, in addition to increased ErbB-3 activation. Since ErbB-3 has impaired kinase activity [2], ErbB-2 is most probably responsible for ErbB-3 phosphorylation.

The specific isoforms of HRG that occur in human breast tumors have not been reported although transcripts for both the α and β isoforms have been detected in cultured breast cancer cells in other experiments not reported here [34,43]. We characterized the specific isoforms of HRG-1 transcripts that occur in the tumors of Wnt-1 transgenic mice (data not shown) and found that the deduced amino acid sequence was highly homologous with the corresponding region of rat (98%) [37] and human (99%) [34] HRG-1α. Since HRG-1α is the major isoform of this ligand expressed in the normal mouse mammary gland, especially during pregnancy [44], our findings indicate that the course of tumor progression did not alter the type of HRG isoform. Pro-HRG immunoreactivity was detected in extracts of mouse mammary tumors and derived cell lines. The 50 kDa-band observed in immunoblots with an antiserum to the extreme C-terminal region of pro-HRG confirms that proteolytic cleavage occurred between the EGF-like domain at the cell exterior face and the transmembrane domain of the ligand

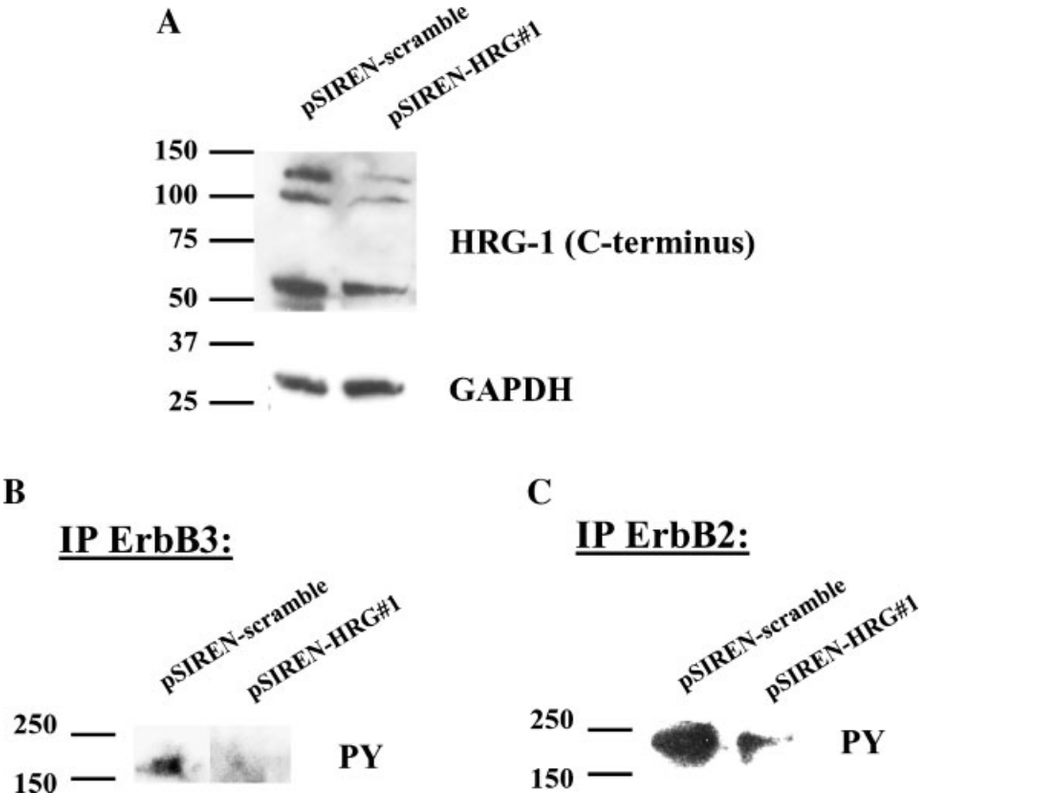

Figure 8. Decrease of heregulin-1 and inhibition of ErbB-2/3 tyrosine phosphorylation in TM-6 cells stably overexpressing a heregulin specific siRNA sequence. (A) TM-6 cells were stably transfected with an expression vector harboring heregulin-1 siRNA (pSIREN-HRG#1) or a scramble sequence. Cell lysates were analyzed for heregulin-1 expression by immunoblotting with the Ab-pro-HRG-CT-1 antiserum. GAPDH was a loading control. (B, C) TM-6 cells were stably transfected with an expression vector harboring heregulin-1 siRNA (pSIREN-HRG#1) or a scramble sequence. Cells were grown in serum-free medium for 24 h and then ErbB-3 (B) or ErbB-2 (C) was immunoprecipitated (IP) from lysates and the blot probed for phosphotyrosine (PY). A representative blot is shown.

precursor, that is, the stalk region of pro-HRG. A potential Lys-Arg cleavage site for a serine protease exists in this region for the α- and β- isoforms of pro-HRG that span the membrane [34]. The detection of the 50 kDa cytoplasmic tail cleavage product in mouse tumors and cell lines is compatible with the presence of the α2a isoform of pro-HRG that has an intact, or extended, C-terminal region [41]. Our data suggest that the cleavage that creates the 50 kDa fragment commonly occurs in mouse mammary tumors. The processing of the membrane-bound pro-HRG-1α occurs similarly for cells in culture and in tumors: in both cases processing results in the formation of the 50 kDa cytoplasmic domain and the active, mature HRG (~45 kDa) ectodomain. The mature 45-kDa fragment of the α isoform containing the EGF-like domain was previously found in conditioned medium of human breast cancer cells [34,45]. In addition to these fragments, lysates of several of the mouse mammary tumors contained smaller bands of HRG-1 immunoreactivity. These may be the result of specific proteolysis or nonspecific cleavage as a result of necrotic processes occurring in the tumors. In TM-6 cell extracts, the predominant cleavage product that contains the EGF-like domain is ~37 kDa. The appearance of bands at 105–110 kDa in Western blots of cell extracts most likely represents the glycosylated intact pro-HRG forms that were previously observed at early time points of pulse-chase labeling experiments with pro-HRG-transfected cells [46]. The relative contribution of cell associated (intact) pro-HRG and secreted, mature HRG forms in ErbB activation within the tumor microenvironment is not known. Since the cleaved rather than the intact form of pro-HRG is the major form in our extracts, it is likely that the mature form activates ErbB-2/ErbB-3. The finding that ErbB-2/3 activation in mammary tumor cells can be inhibited with an antiserum targeting the EGF-like domain of HRG-1 supports the notion that the ligand is secreted or at the cell surface before it interacts with the ErbB-2/ErbB-3 heterodimer. Mature HRG (45 kDa) or other truncated versions of HRG containing the EGF-like domain were previously shown to have bioactivity in vitro and in vivo [47,48].

The cell lines evaluated for ErbB-3 phosphorylation were constitutively activated and refractory to exogenous HRG-1 except for the non-tumorigenic

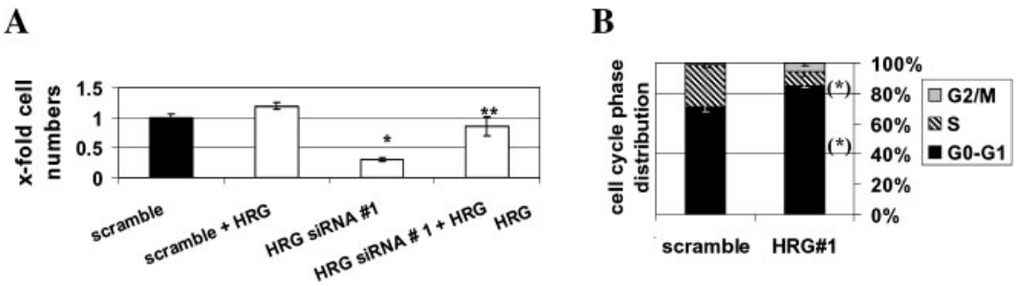

Figure 9. TM-6 cells were stably transfected with an expression vector harboring heregulin-1 siRNA (pSIREN-HRG#1) or a scramble sequence. Cells were seeded in triplicates at a density of 2.2×10^5 per 35-mm dish. After 1 d, cells were washed twice and re-fed. (A) After incubation for 6 d in medium containing 0.5% FBS in the absence or presence of 100 ng/mL heregulin-1β (HRG), cells were detached with trypsin and counted. Changes in cell numbers were calculated and compared with the respective untreated controls. Data are summarized from at least two experiments with three individual data points each; bars represent SE. (*) Significantly different from control-transfected cells; $P < 0.0001$. (**) Significantly different from untreated TM-6-pSIREN-HRG#1 cells; $P = 0.0471$. (B) Cells were grown for 3 d in serum-free medium, then detached with trypsin and fixed in ice-cold ethanol. DNA content was analyzed by flow cytometry after staining with propidium iodide. The data are summarized from two separate trials; bars represent SD. (*) Significantly different from control-transfected cells; G0–G1: $P = 0.02$, S: $P = 0.01$.

COMMA-D cells, which appeared to have less endogenous HRG. Endogenous HRG-1 is cleaved at the cell surface, which may create favorable conditions for binding to and activating ErbB-2/ErbB-3. This may account for why exogenous HRG was generally ineffective in our cell culture studies. When we overexpressed ErbB-3 in mammary epithelial cell lines, total ErbB-3-P-Tyr was also increased. This finding supports the notion that the ErbB-3 present in the parental cancer cell lines is already maximally stimulated. Since ErbB-3 overexpression also increased ErbB-3-P-Tyr in the HRG-responsive COMMA-D cells, ErbB-3 overexpression seems to facilitate its stimulation by exogenous or endogenous HRG.

The fact that the ErbB-1 inhibitor PD153035 markedly reduced ErbB-2 phosphorylation, but not ErbB-3 phosphorylation, suggests that ErbB-1 does not contribute to constitutive ErbB-3 phosphorylation, at least within the context of the cells examined. PD153035 inhibits the ligand (EGF)-stimulated phosphorylation of ErbB-1 [49] and ErbB-2 [50]. The PD153035 did not inhibit the constitutive Tyr-phosphorylation of ErbB-1 in TM-6 cells. This might be explained by the interactions of this receptor with ErbB-2. ErbB-1/ErbB-2 heterodimers are preferred over ErbB-1/ErbB-1 homodimers, and, in the presence of the EGF ligand, ErbB-1 can phosphorylate ErbB-2 and vice versa [51]. Perhaps, under our cell conditions, ErbB-2 is the major substrate (receptor) for the ErbB-1 kinase and only minimal kinase activity resulted in autophosphorylation of ErbB-1. This would account for PD153035 inhibiting ErbB-2, but not ErbB-1 phosphorylation. It is also possible that other (non-ErbB) kinases, for example c-src, targeted ErbB-1 (summarized in Biscardi et al., 2000 [52]).

Conflicting data have been reported regarding the influence of ErbB-2 expression on HRG levels: One study implied a negative correlation between HRG-1 and ErbB-2 expression [53]. In contrast, another study showed induction of HRG transcripts as a result of c-ErbB-2 overexpression [54]. We found HRG transcripts (by RT-PCR) or protein (by Western blots and immunohistochemistry) in mammary tumors or cells that originated from transgenic MMTV-Neu (Wt or activated) mice. HRG-1 expression was not altered when COMMA-D or TM-6 cells were engineered to overexpress ErbB-2. Also, we saw no relationship between ErbB-3 and HRG-1 expression in mammary epithelial tumors, and in none of the mammary epithelial cell lines that we investigated did ErbB-3 overexpression significantly alter HRG-1 levels. Thus, we conclude that HRG expression is not directly regulated by ErbB-2 or ErbB-3 in the experimental samples evaluated. We did find, though, that ErbB-2 positively regulates ErbB-3 expression in mouse epithelial cells. This phenomenon was previously observed in several human breast cell lines [25].

Although we failed to detect activated ErbB-2/ErbB-3 in extracts of the adult mouse mammary gland, we cannot rule out with certainty that these ErbBs are not functional in the normal virgin gland epithelium. Some cells exhibited immunoreactivity for pro-HRG and ErbB-3. A previous study showed that ErbB activation in the normal subadult mammary gland can be hormonally regulated [9]. Few studies, so far, have directly shown the importance of endogenous HRG for ErbB-2/3 activation in mammary epithelial cells. MMTV-NRG (NDFβ2c) transgenic female mice, bred to maximize expression of the transgene, develop mammary adenocarcinomas at a median age of 12 months; a cell line established from this transgenic mouse displayed constitutive activation of ErbB-3 [28]. In another study, HRG-1 stably expressed in the ErbB-2/ErbB-4-positive MCF-7 cells increased the proliferation rate [55]. When injected into mice, the cells formed tumors, and preneoplastic changes occurred in the surrounding mammary gland tissue of the host [27]. When the

human MDA-MB-435 breast cancer cells transfected with a HRG expression vector were injected into nude mice, they showed an increased tumor growth rate compared with control-transfected cells [26]. Li et al. [56] demonstrated that HRG levels in MCF10A cells increased with the extent of malignancy, and that this transition was associated with an apparent HRG-ErbB-2/ErbB-3 autocrine loop that provided a proliferative stimulus to these cells. In another study, a polyclonal antiserum to the N-terminal region of the HRG EGF-like domain inhibited the in vitro growth pattern and motility of three human breast cancer cell lines constitutively expressing this ligand [57]. In a related study, inhibition of HRG synthesis in MDA-MB-231 cells was achieved with an antisense RNA expression vector. In addition to suppressing anchorage-dependent and-independent cell growth, as well as chemoinvasion in vitro, the antisense vector suppressed the tumorigenicity and metastasis of the cells in athymic nude mice [58]. However, compelling evidence was not offered in this study to show that inhibition of HRG reduced ErbB-2/ErbB-3 activation. We do show in our study that TM-6 cells stably expressing a siRNA sequence targeting HRG-1 are strongly growth suppressed. Both anti-HRG antibodies and HRG siRNA (transiently transfected oligonucleotides and stably expressed) reduce constitutive phosphorylation of ErbB-2 and ErbB-3 in these cells, similar to cells expressing a dominant-negative ErbB-3 receptor [59] or HRG-antisense cDNA [58]. It is likely that the reduction in ErbB-2/ErbB-3 activation observed with the HRG siRNA contributed to the reduced proliferation rate because addition of the ligand restored the growth rate to control values. Based on these observations, we propose that the proliferative or oncogenic potential of the ErbB-2/ErbB-3 heterodimer is highly dependent on the coexpression of and constitutive activation by HRG in a subset of breast cancer cells, but that coexpression in itself is not sufficient to drive autonomous cell growth. ErbB-2 and ErbB-3 are constitutively activated in most mammary tumor cells. A series of events may take place in the course of tumorigenesis that removes the necessity for hormonal regulation in ErbB-2/3 activation. Inappropriate expression of HRG-1 may contribute to that phenomenon. The failure of the siRNA approach to drastically reduce HRG-1 synthesis might be due, in part, to the silencing capability of the sequence chosen. The downregulation achieved with transient transfection could have been hampered by the long half-life of pro-HRG or by a suboptimal transfection-efficiency because of toxicity of the transfection agent. A drawback of the stable construct was that the pSIREN vector allowed for a deregulation of the promoters driving the RNAi sequence and the puromycin-resistance. Since neither the siRNA nor the antibody method completely abolished ErbB-3 phosphorylation, it cannot be excluded that there are other unknown ligands contributing to ErbB-3-phosphorylation.

Taken together, our results indicate that constitutive HRG-1 expression, occurring with a high proclivity in the epithelium of mouse mammary tumors, can be critical for activation of ErbB-2/ErbB-3 receptors expressed in the same cells. There is a subset of breast tumor cells that are highly dependent for their proliferative behavior on endogenous or exogenous HRG, implying that blocking this pathway may be beneficial for breast cancer patients whose tumors coexpress ErbB-2 and ErbB-3. However, more extensive studies of clinical specimens as to the extent of the coexpression of HRG and ErbB-2/ErbB-3 are needed. Currently, our lab is extending the study to determine additional biological effects that are driven by endogenous HRG-1 that might be relevant for tumor cell growth and metastasis.

ACKNOWLEDGMENTS

We thank Dr. Barbara Davis and Ghanta Rao for mammary tumors from MMTV-Wnt-1 and MMTV-c-Neu (activated) transgenic mice, respectively, and Dr. Darlene Dixon for obtaining mammary tumors from mice that were part of a chemical carcinogenesis study conducted by The National Toxicology Program. The sequencing reactions were performed by the NIEHS sequencing core. We also thank Gail Grossman from the Immunotechnology and Histochemistry Core of the Laboratories for Reproductive Biology at UNC Chapel Hill for technical assistance, Dr. Carl Bortner for help with the Flow Cytometry analysis, Dr. Jeanelle Martinez for suggestions concerning the real-time PCR reactions, Dr. Grace Kissling for the statistical analysis, Dr. Diane Klotz for helpful suggestions, and Dr. John Roberts and Sylvia C. Hewitt for reviewing the manuscript.

REFERENCES

1. Lupu R, Cardillo M, Harris L, Hijazi M, Rosenberg K. Interaction between erbB-receptors and heregulin in breast cancer tumor progression and drug resistance. Semin Cancer Biol 1995;6:135–145.
2. Guy PM, Platko JV, Cantley LC, Cerione RA, Carraway KL 3rd. Insect cell-expressed p180erbB3 possesses an impaired tyrosine kinase activity. Proc Natl Acad Sci USA 1994;91:8132–8136.
3. Riese DJ 2nd, Stern DF. Specificity within the EGF family/ErbB receptor family signaling network. Bioessays 1998;20:41–48.
4. Pinkas-Kramarski R, Alroy I, Yarden Y. ErbB receptors and EGF-like ligands: Cell lineage determination and oncogenesis through combinatorial signaling. J Mam Gland Biol Neoplasia 1997;2:97–107.
5. Chen X, Levkowitz G, Tzahar E, et al. An immunological approach reveals biological differences between the two NDF/heregulin receptors, ErbB-3 and ErbB-4. J Biol Chem 1996;271:7620–7629.
6. Wallasch C, Weiss FU, Niederfellner G, Jallal B, Issing W, Ullrich A. Heregulin-dependent regulation of HER2/neu oncogenic signaling by heterodimerization with HER3. Embo J 1995;14:4267–4275.

7. Sliwkowski MX, Schaefer G, Akita RW, et al. Coexpression of erbB2 and erbB3 proteins reconstitutes a high affinity receptor for heregulin. J Biol Chem 1994;269:14661–14665.
8. Holbro T, Beerli RR, Maurer F, Koziczak M, Barbas CF 3rd, Hynes NE. The ErbB2/ErbB3 heterodimer functions as an oncogenic unit: ErbB2 requires ErbB3 to drive breast tumor cell proliferation. Proc Natl Acad Sci USA 2003;100:8933–8938.
9. Sebastian J, Richards RG, Walker MP, et al. Activation and function of the epidermal growth factor receptor and erbB-2 during mammary gland morphogenesis. Cell Growth Differ 1998;9:777–785.
10. Carraway KL 3rd, Burden SJ. Neuregulins and their receptors. Curr Opin Neurobiol 1995;5:606–612.
11. Soltoff SP, Carraway KL 3rd, Prigent SA, Gullick WG, Cantley LC. ErbB3 is involved in activation of phosphatidylinositol 3-kinase by epidermal growth factor. Mol Cell Biol 1994; 14:3550–3558.
12. Hynes NE, Stern DF. The biology of erbB-2/neu/HER-2 and its role in cancer. Biochim Biophys Acta 1994;1198:165–184.
13. Siegel PM, Ryan ED, Cardiff RD, Muller WJ. Elevated expression of activated forms of Neu/ErbB-2 and ErbB-3 are involved in the induction of mammary tumors in transgenic mice: Implications for human breast cancer. Embo J 1999; 18:2149–2164.
14. Bieche I, Onody P, Tozlu S, Driouch K, Vidaud M, Lidereau R. Prognostic value of ERBB family mRNA expression in breast carcinomas. Int J Cancer 2003;106:758–765.
15. Bodey B, Bodey B, Jr., Groger AM, et al. Clinical and prognostic significance of the expression of the c-erbB-2 and c-erbB-3 oncoproteins in primary and metastatic malignant melanomas and breast carcinomas. Anticancer Res 1997; 17:1319–1330.
16. Kraus MH, Issing W, Miki T, Popescu NC, Aaronson SA. Isolation and characterization of ERBB3, a third member of the ERBB/epidermal growth factor receptor family: Evidence for overexpression in a subset of human mammary tumors. Proc Natl Acad Sci USA 1989;86:9193–9197.
17. Alimandi M, Romano A, Curia MC, et al. Cooperative signaling of ErbB3 and ErbB2 in neoplastic transformation and human mammary carcinomas. Oncogene 1995;10: 1813–1821.
18. Guy CT, Webster MA, Schaller M, Parsons TJ, Cardiff RD, Muller WJ. Expression of the neu protooncogene in the mammary epithelium of transgenic mice induces metastatic disease. Proc Natl Acad Sci USA 1992;89: 10578–10582.
19. Zhou H, Liu L, Lee K, et al. Lung tumorigenesis associated with erb-B-2 and erb-B-3 overexpression in human erb-B-3 transgenic mice is enhanced by methylnitrosourea. Oncogene 2002;21:8732–8740.
20. Bacus SS, Gudkov AV, Zelnick CR, et al. Neu differentiation factor (heregulin) induces expression of intercellular adhesion molecule 1: Implications for mammary tumors. Cancer Res 1993;53:5251–5261.
21. Guerra-Vladusic FK, Scott G, Weaver V, et al. Constitutive expression of Heregulin induces apoptosis in an erbB-2 overexpressing breast cancer cell line SKBr-3. Int J Oncol 1999;15:883–892.
22. Le XF, Vadlamudi R, McWatters A, et al. Differential signaling by an anti-p185(HER2) antibody and heregulin. Cancer Res 2000;60:3522–3531.
23. Daly JM, Jannot CB, Beerli RR, Graus-Porta D, Maurer FG, Hynes NE. Neu differentiation factor induces ErbB2 down-regulation and apoptosis of ErbB2-overexpressing breast tumor cells. Cancer Res 1997;57:3804–3811.
24. Normanno N, Ciardiello F, Brandt R, Salomon DS. Epidermal growth factor-related peptides in the pathogenesis of human breast cancer. Breast Cancer Res Treat 1994;29: 11–27.
25. Aguilar Z, Akita RW, Finn RS, et al. Biologic effects of heregulin/neu differentiation factor on normal and malignant human breast and ovarian epithelial cells. Oncogene 1999;18:6050–6062.
26. Meiners S, Brinkmann V, Naundorf H, Birchmeier W. Role of morphogenetic factors in metastasis of mammary carcinoma cells. Oncogene 1998;16:9–20.
27. Atlas E, Cardillo M, Mehmi I, Zahedkargaran H, Tang C, Lupu R. Heregulin is sufficient for the promotion of tumorigenicity and metastasis of breast cancer cells in vivo. Mol Cancer Res 2003;1:165–175.
28. Krane IM, Leder P. NDF/heregulin induces persistence of terminal end buds and adenocarcinomas in the mammary glands of transgenic mice. Oncogene 1996;12:1781–1788.
29. Tsukamoto AS, Grosschedl R, Guzman RC, Parslow T, Varmus HE. Expression of the *int-1* gene in transgenic mice is associated with mammary gland hyperplasia and adenocarcinomas in male and female mice. Cell 1988;55:619–625.
30. Muller WJ, Sinn E, Pattengale PK, Wallace R, Leder P. Single-step induction of mammary adenocarcinoma in transgenic mice bearing the activated c-neu oncogene. Cell 1988;54: 105–115.
31. Reilly RT, Gottlieb MB, Ercolini AM, et al. HER-2/neu is a tumor rejection target in tolerized HER-2/neu transgenic mice. Cancer Res 2000;60:3569–3576.
32. Kittrell FS, Oborn CJ, Medina D. Development of mammary preneoplasias in vivo from mouse mammary epithelial cell lines in vitro. Cancer Res 1992;52:1924–1932.
33. Danielson KG, Oborn CJ, Durban EM, Butel JS, Medina D. Epithelial mouse mammary cell line exhibiting normal morphogenesis in vivo and functional differentiation in vitro. Proc Natl Acad Sci USA 1984;81:3756–3760.
34. Holmes WE, Sliwkowski MX, Akita RW, et al. Identification of heregulin, a specific activator of p185erbB2. Science 1992; 256:1205–1210.
35. Laemmli UK. Cleavage of structural proteins during the assembly of the head of bacteriophage T4. Nature 1970;227: 680–685.
36. Balana ME, Lupu R, Labriola L, Charreau EH, Elizalde PV. Interactions between progestins and heregulin (HRG) signaling pathways: HRG acts as mediator of progestins proliferative effects in mouse mammary adenocarcinomas. Oncogene 1999;18:6370–6379.
37. Wen D, Peles E, Cupples R, et al. Neu differentiation factor: A transmembrane glycoprotein containing an EGF domain and an immunoglobulin homology unit. Cell 1992;69:559–572.
38. Friedman J, Weissman I. Two cytoplasmic candidates for immunophilin action are revealed by affinity for a new cyclophilin: One in the presence and one in the absence of CsA. Cell 1991;66:799–806.
39. Sambrook J, Fritsch EF, Maniatis T. Molecular Cloning: A laboratory manual. New York: Cold Spring Harbor Laboratory Press; 1989. pp 1.82–1.84.
40. Bortner CD, Cidlowski JA. Caspase independent/dependent regulation of K(+), cell shrinkage, and mitochondrial membrane potential during lymphocyte apoptosis. J Biol Chem 1999;274:21953–21962.
41. Wen D, Suggs SV, Karunagaran D, et al. Structural and functional aspects of the multiplicity of Neu differentiation factors. Mol Cell Biol 1994;14:1909–1919.
42. Tzahar E, Waterman H, Chen X, et al. A hierarchical network of interreceptor interactions determines signal transduction by Neu differentiation factor/neuregulin and epidermal growth factor. Mol Cell Biol 1996;16:5276–5287.
43. Normanno N, Kim N, Wen D, et al. Expression of messenger RNA for amphiregulin, heregulin, and cripto-1, three new members of the epidermal growth factor family, in human breast carcinomas. Breast Cancer Res Treat 1995;35:293–297.
44. Yang Y, Spitzer E, Meyer D, et al. Sequential requirement of hepatocyte growth factor and neuregulin in the morpho-

genesis and differentiation of the mammary gland. J Cell Biol 1995;131:215–226.
45. Ethier SP, Langton BC, Dilts CA. Growth factor-independent proliferation of rat mammary carcinoma cells by autocrine secretion of neu-differentiation factor/heregulin and transforming growth factor-alpha. Mol Carcinog 1996;15:134–143.
46. Burgess TL, Ross SL, Qian YX, Brankow D, Hu S. Biosynthetic processing of neu differentiation factor. Glycosylation trafficking, and regulated cleavage from the cell surface. J Biol Chem 1995;270:19188–19196.
47. Harris A, Adler M, Brink J, et al. Homologue scanning mutagenesis of heregulin reveals receptor specific binding epitopes. Biochem Biophys Res Commun 1998;251:220–224.
48. Weinstein EJ, Leder P. The extracellular region of heregulin is sufficient to promote mammary gland proliferation and tumorigenesis but not apoptosis. Cancer Res 2000;60: 3856–3861.
49. Fry DW, Kraker AJ, McMichael A, et al. A specific inhibitor of the epidermal growth factor receptor tyrosine kinase. Science 1994;256:1093–1095.
50. Nielsen UB, Cardone MH, Siskey AJ, MacBeath G, Sorger PK. Profiling receptor tyrosine kinase activation by usiing Ab microarrays. PNAS 2003;2003:9330–9335.
51. Qian X, LeVea CM, Freeman JK, Dougall WC, Greene MI. Heterodimerization of epidermal growth factor receptor and wild-type or kinase-deficient Neu: A mechanism of interreceptor kinase activation and transphosphorylation. PNAS 1994;91:1500–1504.
52. Biscardi JS, Ishizawar RC, SIlva CM, Parsons SJ. Tyrosine kinase signalling in breast cancer. Epidermal growth factor receptor and c-Src interactions in breast cancer. Breast Cancer Res 2000;2:203–210.
53. deFazio A, Chiew YE, Sini RL, Janes PW, Sutherland RL. Expression of c-erbB receptors, heregulin and oestorgen receptor in human breast cell lines. Int J Cancer 2000; 87:487–498.
54. Mincione G, Bianco C, Kannan S, et al. Enhanced expression of heregulin in c-erb B-2 and c-Ha-ras transformed mouse and human mammary epithelial cells. J Cell Biochem 1996; 60:437–446.
55. Lupu R, Cardillo M, Cho C, et al. The significance of heregulin in breast cancer tumor progression and drug resistance. Breast Cancer Res Treat 1996;38:57–66.
56. Li Q, Ahmed SL, Loeb JA. Development of an autocrine neuregulin signaling loop with malignant transformation of human breast epithelial cells. Cancer Res 2004;64:7078–7085.
57. Hijazi MM, Thompson EW, Tang C, et al. Heregulin regulates the actin cytosceleton and promotes invasive propoerties in breast cancer cell lines. Int J Oncol 2000;17:629–641.
58. Tsai MS, Shamon-Taylor LA, Mehmi I, Tang CK, Lupu R. Blockage of heregulin expression inhibits tumorigenicity and metastasis of breast cancer. Oncogene 2003;22:761–768.
59. Ram TG, Schelling ME, Hosick HL. Blocking HER-2/HER-3 function with a dominant negative form of HER-3 in cells stimulated by heregulin and in breast cancer cells with HER-2 gene amplification. Cell Growth Differ 2000;11:173–183.